Research Paper

Changes of articular cartilage and subchondral bone after extracorporeal shockwave therapy in osteoarthritis of the knee

Ching-Jen Wang[1,2]✉*, Jai-Hong Cheng[1]*, Wen-Yi Chou[2], Shan-Ling Hsu[1,2], Jen-Hung Chen[2] and Chien-Yiu Huang[1,2]

1. Center for Shockwave Medicine and Tissue Engineering;
2. Department of Orthopedic Surgery, Section of Sports Medicine;
3. Kaohsiung Chang Gung Memorial Hospital and Chang Gung University College of Medicine, Kaohsiung, Taiwan.

*Equal contribution

✉ Corresponding author: w281211@adm.cgmh.org.tw; Tel.: 886-7-733-5279; Fax: 886-7-733-5515

Abstract

We assessed the pathological changes of articular cartilage and subchondral bone on different locations of the knee after extracorporeal shockwave therapy (ESWT) in early osteoarthritis (OA). Rat knees under OA model by anterior cruciate ligament transaction (ACLT) and medial meniscectomy (MM) to induce OA changes. Among ESWT groups, ESWT were applied to medial (M) femur (F) and tibia (T) condyles was better than medial tibia condyle, medial femur condyle as well as medial and lateral (L) tibia condyles in gross osteoarthritic areas (p<0.05), osteophyte formation and subchondral sclerotic bone (p<0.05). Using sectional cartilage area, modified Mankin scoring system as well as thickness of calcified and un-calcified cartilage analysis, the results showed that articular cartilage damage was ameliorated and T+F(M) group had the most protection as compared with other locations (p<0.05). Detectable cartilage surface damage and proteoglycan loss were measured and T+F(M) group showed the smallest lesion score among other groups (p<0.05). Micro-CT revealed significantly improved in subchondral bone repair in all ESWT groups compared to OA group (p<0.05). There were no significantly differences in bone remodeling after ESWT groups except F(M) group. In the immunohistochemical analysis, T+F(M) group significant reduced TUNEL activity, promoted cartilage proliferation by observation of PCNA marker and reduced vascular invasion through observation of CD31 marker for angiogenesis compared to OA group (P<0.001). Overall the data suggested that the order of the effective site of ESWT was T+F(M) ≧ T(M) > T(M+L) > F(M) in OA rat knees.

Key words: shockwave, osteoarthritis, cartilage histopathology, subchondral bone, rats.

Introduction

Osteoarthritis (OA) of the knee is a common orthopedic disorder that causes pain and functional disability in daily activities. OA is a multifactorial process including age, obesity, injury, overuse, and infection [1]. OA knee has been considered primarily an articular cartilage disease caused by cartilage degradation and loss. However, OA is usually observed the changes in the subchondral and periarticular bone with pathological sclerosis, bone cyst and osteophyte [2, 3]. The correlation of the subchondral bone damages and the development of OA are still argued [4-6]. Current reports indicate that increased bone turnover is observed in patients with osteoarthritis [7-10]. Subchondral bone stiffness is measured and suggests contributing in cartilage deterioration and changes of OA knee [11]. One study showed subchondral bone damage in the early stage of knee OA and observed bone sclerosis in the late

stage of a dog model [7]. During the OA progressed, increased bone resorption results in reduction of subchondral bone volume, increased sclerotic bone and formation of periarticular osteophytes [5, 6, 12].

The subchondral bone shows a significant leading role that causes secondary changes of the articular cartilage in knee OA [4-6, 10, 12]. Muraoka and colleagues showed that subchondral bone formation is the key role before the onset of cartilage damage in Hartley guinea pigs and it is significant in the development of OA disease [10]. Brama and colleagues reported that microarchitecture of subchondral bone supported the overlying articular cartilage and involved in osteochondral disease [13]. The increased subchondral bone stiffness decreased the ability of the knee joint to scatter the loading forces within the joint. Therefore, the serious consequence increases the force load on the overlying articular cartilage to accelerate the cartilage damage and OA changes over time [7, 14]. Further, the researchers reported the significant role of subchondral bone in the initiation and progression of knee OA changes because the functional integrity of the articular cartilage depends upon the mechanical properties of the subchondral bone [11]. The strategic changes in the management of early knee osteoarthritis have occurred by the paradigm shift of the initial focus of treatment from the articular cartilage to the subchondral bone [15-17].

Many studies reported that ESWT has the positive effects in osteoarthritis of knee in different kind of animals [18-22]. Dahlberg and colleagues showed that ESWT improved lameness, peak vertical force, and range of motion as compared with the control without ESWT in dogs [18]. Frisbie and colleagues reported that ESWT improved the degrees of lameness in horse, but no disease modifying effects as evidenced by synovial fluid analysis, synovial membrane or cartilage [19]. Mueller and colleagues demonstrated that the limb function of dogs with the difference in ground reaction force between two limbs were improved after ESWT in hip osteoarthritis [20]. Ochiai et al showed that ESWT is a efficient treatment for knee OA with improvement in walking ability and the reduction of calcitonin gene-related peptide in dorsal root ganglion neurons innervating the knee [21]. Revenaugh et al recommended that ESWT was a valuable adjunct for the treatment of equine OA [22]. All these authors reported that ESWT was effective in OA knee, but none showed the best location of ESWT application for OA knees. The current study expanded and further investigated the pathological changes in articular cartilage and subchondral bone after ESWT at various locations in OA knee.

Materials and Methods

Care of animals

Forty-eight Sprague-Dawley rats (BioLasco, Taipei, Taiwan) were used in this experiment. The IACUC protocol of the animal study was approved by the Animal Care Committee of Kaohsiung Chang Gung Memorial Hospital. The reference number is 2012041001. The animals were maintained at the laboratory Animal Center for 1 week before experiment. They were housed at $23 \pm 1°$ C with a 12-hour light and dark cycle and given food and water.

Shockwave application

The optimal dose of ESWT in small animals was examined in previous studies [23, 24]. ESWT was performed in one week after knee surgery when the surgical wound healed. The animals were sedated with 1:1 volume mixture of Rompun (5 mg/Kg) + Zoletil (20 mg/Kg) while receiving ESWT. The source of shockwave was from an OssaTron (Sanuwave, Alpharetta, GA, USA). Ultrasound guide was used to precisely tracking of the focus of shockwave application at the respective locations of different groups. Each location was treated with 800 impulses of shockwave at 0.22 mJ/mm² energy flux density in one single session.

The study design

The rats were divided into 6 groups with 8 rats in each group. Sham group was the control that received sham ACLT and MM. OA group was the osteoarthritis group that received ACLT and MM, but no shockwave treatment. T(M) group received ACLT and MM and ESWT to medial (M) tibia (T) condyle. F(M) group received ACLT+MM and ESWT to the medial femoral (F) condyle. T+F (M) group was received ACLT+MM and ESWT to medial femoral condyle and tibia condyle of the knee respectively. T(M+L) group received ACLT+MM and ESWT to medial tibia condyle and lateral (L) tibia condyle respectively.

The animals were sacrificed at 12 weeks. The experimental design of this study was shown in Supplemental Figure 1. The evaluation parameters included the severity of gross osteoarthritis lesion score and osteophyte lesion area (%), Safranin-O stain for modified Mankin score and the cartilage areas, un-calcified and calcified cartilage thickness, histopathology of cartilage. The micro-CT for bone volume, bone porosity, trabecular thickness and numbers, and immunohistochemical analysis for TUNEL, PCNA and CD31 expressions.

Animal model of osteoarthritis

The left knee was prepared in surgically sterile fashion. Through medial parapatellar mini-arthrotomy, the ACL fibers were transected with a scalpel, and medial meniscectomy was performed by excising the entire medial meniscus. The knee joint was irrigated and the incision was closed. Prophylactic antibiotic with ampicillin 50 mg/Kg body weight was given for 5 days after surgery. Postoperatively, the animals were returned to the housing cage and cared for by a veterinarian. The surgical site and the animal activities were observed daily.

Histopathological scores of osteoarthritic lesion area measurement

The gross pathological lesions with arthritic changes on femoral condyle and tibia plateau were identified and quantified separately by the semiquantitative scale under a magnification scope (Carl Zeiss, Oberkochen, Germany). The severity of joint surface damage was categorized and scored as follows: (a). Intact surface or normal in appearance = 0 point, (b). Surface rough with minimal fibrillation or a slight yellowish discoloration =1 point, (c). Cartilage erosion extending into the superficial or middle layers = 2.points, (d). Cartilage erosion extending into the deep layer = 3 points, (e). Complete cartilage erosion with subchondral bone exposed = 4 points. The average scores were obtained by summing the cartilage scores of the lesions in femur condyle and tibia plateau cartilage in eight knees of each group.

For arthritic area measurements, the total surfaces of osteophyte and lesion on medial tibia plateaus were manually traced by using imageJ software program (NH, Bethesda, MD, USA) and areas were determined by using the ImagePro Plus analysis program (Media cybernetics Inc, Rockville, MD, USA). The percentage of osteophyte lesion areas was calculated as osteophyte and lesion areas divided by medial tibia plateau area × 100%.

Modified Mankin score and cartilage area measurement

The degenerative changes of the cartilage were graded histologically by using the modified Mankin Score to assess the severity of OA via Safranin O stain. The scoring system included the analytical factors of cartilage surface damage, loss of celluarlity, loss of matrix staining, loss of tidemark integrity and proportions of lesion site. The modified Mankin scores were obtained on a 0 to 33 scale by addition of the analytical factors [25]. For cartilage area measurement, eight non-consecutive sections, which were obtained at 100 µm intervals, were measured per

knee joint. Two reference points 1 and 2 with a distance of 2.00 µm, which covers the majority of cartilage layer was automatically generated at the margin of cartilage. The width of cartilage at a reference point was measured and the area was automatically calculated by image software [26-29].

Measurements of un-calcified and calcified cartilage thickness

Cartilage thickness was measured by eight non-consecutive sections, which were obtained at 100 µm interval. Safranin-O stain provided layer discrimination between un-calcified (UCC) and calcified cartilage (CC). Cartilage areas were automatically calculated by imageJ software as described, and the average thickness was then determined as areas divided by the length. The UCC and CC thickness were reconfirmed by measuring individual cartilage point-to-point distance by averaging six measurements per sample.

Micro-CT examination and bone mineral density

The proximal part of the tibia and the distal part of the femur were scanned with micro-CT scanner (Skyscan 1076; Skyscan, Luxembourg, Gelgium) with isotopic boxel size of 36 x 36 x 36 µm as previously described. The X-rays voltage was set at 100 Kv, and the current at 100 µA. The X-ray projections were obtained at 0.75 degrees angular step with a scanning angular range of 180 degrees. Reconstruction of the image slices were performed with NRecon software (Skyscan) and the process generated a series of planar transverse gray value images. The volume of interest (VOI) of bone morphometry was selected with a semiautomatic contouring method by Skyscan CT-analyser software. Three-dimensional cross-sectional images were generated by CTVol v 2.0 software. The micro-CT parameters of % bone volume and porosity, trabecular thickness and number, and sclerotic bone volume in subchondral compartment regions were determined. The bone mineral density values with the region of interest (ROI) in respective tibia and femur condyles were measured by using dual-energy X-ray absorptiometry (DEXA, Hologic QDR 4500 W, Hologic, Bedford, MA, USA) at pixel areas resolution at 640 µm².

Immunohistochemical analysis

The harvested knee specimens were fixed in 4% PBS buffered formaldehyde for 48 hours and decalcified in 10% PBS-buffered EDTA solution. Decalcified tissues were embedded in paraffin wax. The specimens were cut longitudinally into 5 μm thick sections and transferred to ploylysine-coated

slides (Thermo Fisher Scientific, Waltham, MA, USA). The TUNEL analysis was accomplished by in Situ Cell Death Detection Kits (Roche Diagnostic, Mannheim, Germany) followed by manufacture instructions. The TUNEL color stains were performed by using NBC/BCIP substrate (Sigma-Aldrich, St. Louis, MO, USA). The immunohistochemical stains were performed by following the protocol provided in the kit (Abcam, Cambridge, MA, USA). The tissue sections were de-paraffinized in xylene, hydrated in graded ethanol, and treated with peroxide block and protein-block reagents. Sections of the specimens were immunostained with the specific antibodies for PCNA (Thermo Fisher) at 1:300 dilution and CD31 (GeneTax, Irvine, CA, USA) at 1:200 for overnight to identify the cell proliferation and vascular invasion into the calcified cartilage. The immunoreactivity in specimens was demonstrated by using a goat anti-rabbit horseradish peroxide (HRP)-conjugated and 3', 3'- diaminobenzendine (DAB), which were provided in the kit. The immunoactivities were quantified from five random areas in three sections of the same specimen by using a Zeiss Axioskop 2 plus microscpe (Carl Zeiss, Gottingen, Germany). All images of each specimen were captured by using a cool CCD camera (Media Cybernaetics, Silver Spring, MD, USA). Images were analysed by manual counting and confirmed by using an image-pro Plus Image-analysis software (Media Cybernetics).

Statistical analysis

SPSS ver. 17.0 (SPSS Inc., Chicago, IL, USA) was used in statistical analysis. Data were expressed as mean ± SD. One-way ANOVA and Tukey tests were used to compare sham group versus T(M), F(M), T+F(M) and T(M+L) groups (designated as $*P < 0.05$ and $**P < 0.001$). One-way ANOVA and Tukey tests were also used to compare OA group versus T(M), F(M), T+F(M) and T(M+L) groups (designated as $^{\#}P < 0.05$ and $^{\#\#}P < 0.001$). The intra-group evaluations of T(M) group versus F(M), T+F(M) and T(M+L) groups were determined by Student's t-test (designated as $^{※}P < 0.05$).

Results

Macroscopic assessment of knee pathology

The gross osteoarthritis lesions of the distal femur condyle and the proximal tibia plateaus were shown in Figures 1A and 1B. OA group showed significantly higher gross pathological lesion score than sham group (Figure 1B; 3.156±0.156 vs 0.156±0.027, p<0.001). ESWT groups significantly reduced the gross pathological lesion score and the lowest scores were noticed in T+F(M) with 50 % reduction in gross pathological lesion score compared to OA group (1.500±0.190 vs 3.156±0.156, p<0.001). The osteophyte area and osteoarthritis lesion score were measured in Figure 1C. The osteophyte area was significantly larger in OA group than sham group (Figure 1C; 72.095±6.932 vs 0.500±0.000, p<0.001). ESWT significantly decreased the osteophyte lesion areas by 49 % of T(M) group (37.062±6.609), 30% of F(M) group (50.068±6.371), 63 % of T+F(M) group (26.867±5.773) and 58 % of T(M+L) group (30.567±7.815) compared to OA group (72.095±6.932, p<0.05 and p<0.001). In Figure 1D, ESWT groups reduced formation of sclerotic bone from 0.7 fold difference of T(M) group (5.652±0.539) to 2.1 fold difference of T+F(M) group (3.495±0.391) except F(M) group (7.728±0.564) compared to OA group (7.259±0.871, p<0.05 and p<0.001). F(M) group showed the increasing sclerotic bone volume as the same with OA group. This indicated that the prevention of sclerotic bone in OA knee was not effectiveness on the medial femur site after ESWT. These results showed the protection of ESWT on T+F(M) was better than others.

Cartilage analysis at different sites after ESWT

Microphotographs of articular cartilage were analysis by Safarine-O stain, sectional cartilage areas and modified Mankin score after ESWT (Figure 2). The sectional cartilage areas were significantly smaller in OA group (0.339±0.158 mm²) relative to sham group (0.873±0.119 mm², p<0.001). ESWT significantly increased the cartilage areas with the largest areas in T(M) group (0.588±0.140 mm²), F(M) group (0.477±0.106 mm²), T+F(M) group (0.721±0.063 mm²) and T(M+L) group (0.621±0.122 mm²) compared to OA group (p<0.05 and p<0.001), and no significant difference was noticed between T(M) group and T(M+L) group (Figure 2B). The modified Mankin score was significantly higher in OA group (26.833±1.249, p<0.001) relative to the sham group (0.666±0.335). ESWT significantly decreased the modified Mankin scores with about 3.6 fold difference from lowest to highest scores in T(M) group (10.500±2.232, p<0.05), F(M) group (18.333±1.706, p<0.05), T+F(M) group (5.667±1.600, p<0.001) and T(M+L) group (9.500±1.258, p<0.05) compared to OA group (Figure 2C). Among ESWT groups, T+F(M) group showed the best protection of cartilage damage than other groups.
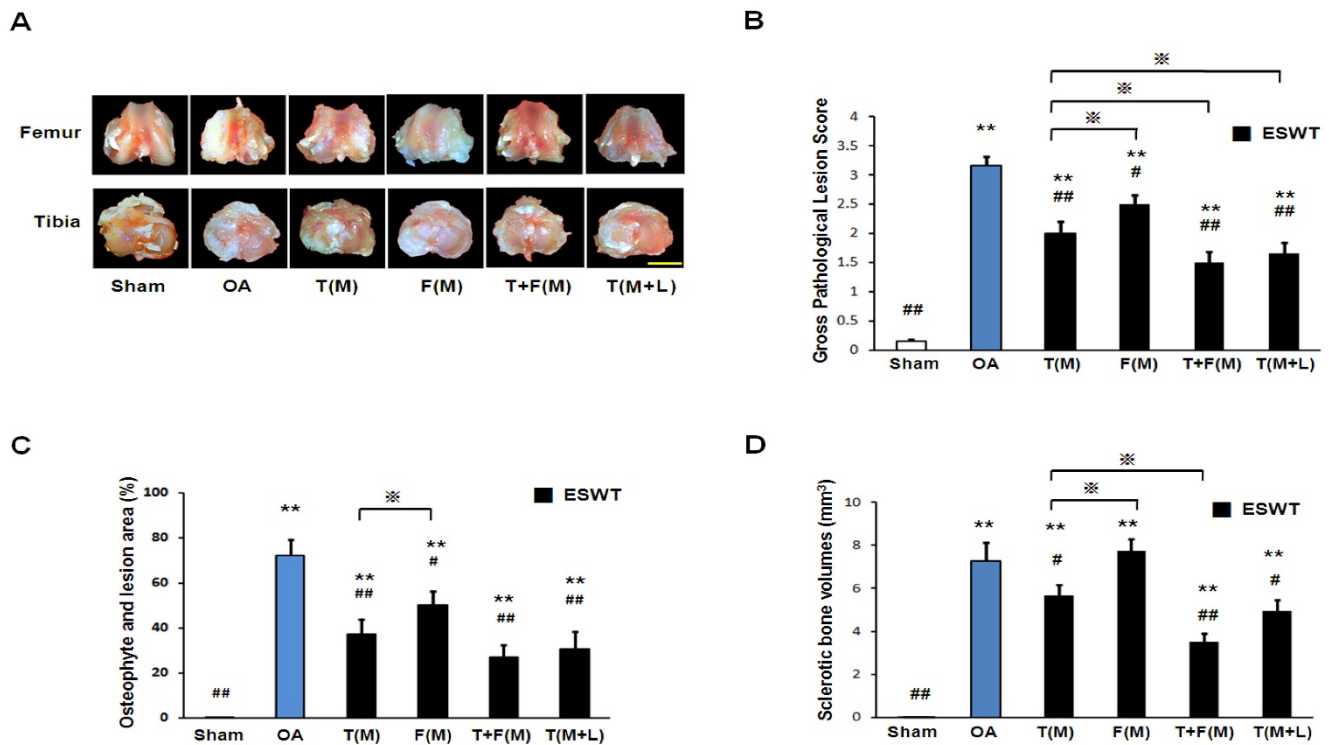
Figure 1. The photographs showed macroscopic pathological osteoarthritic lesions of knee including the areas of osteophyte formation. (A) The knee photos demonstrated the gross pathological osteoarthritic lesions in distal femur and proximal tibia. The scale bar represented 5 mm. (B), (C) and (D) showed the gross appearance of OA lesion, osteophyte and lesion area as well as sclerotic bone volumes (n = 8 in each groups). The ESWT groups showed significantly lower lesion scores as compared to OA group and sham group. Amongst EWST groups, T+F(M) showed the lowest lesion score than other groups. **P < 0.001 compared to sham group. #P < 0.05, ##P< 0.001 compared to OA group. ※P < 0.05 compared to T(M).
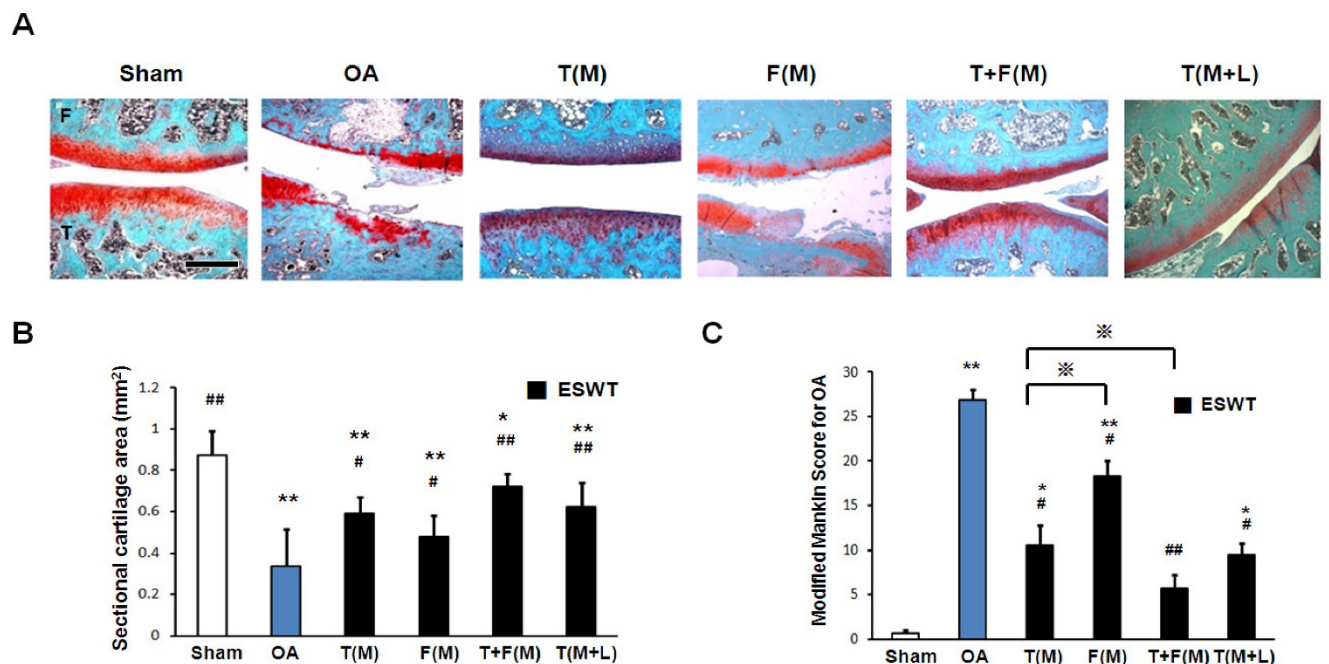

Figure 2. The microphotographs of the knee showed articular cartilage degradation of the knee after ESWT. (A) Microphotographs of articular cartilage demonstrated cartilage damage in OA knee changes. The scale bar represented 200 μm. (B) and (C) showed graphic illustrations of cartilage area and modified Mankin score in histopathological examination. The ESWT groups showed significant increase in cartilage area and decrease in modified Mankin scoreas compared to OA group and sham group. Amongst ESWT groups, T+F(M) group showed the most dramatic changes than other groups. *P < 0.05, **P < 0.001 compared to sham group. #P < 0.05, ##P < 0.001 compared to OA group. ※P< 0.05 compared to T(M) group. All rats were n = 8.

The changes of the un-calcified and calcified cartilages after ESWT

The measurements of cartilage thickness were shown in Figure 3. The pathologies of OA knee were observed by erosion of the cartilage surface, loss of proteoglycan from the articular cartilage, and formation of chondrocyte clusters. The cartilage between the un-calcified and the calcified regions were shown by Safarine-O stain in Figure 3A. The quantitative data of the un-calcified and calcified cartilage thickness were measured individually (Figures 3B and 3C). The un-calcified cartilage thickness significantly decreased in OA group (42.375 ±34.932 μm) relative to the sham group (295.625± 53.407 μm, p<0.001). ESWT significantly increased the un-calcified cartilage thickness with the most thickness in T(M) group (114.125 ± 35.167 μm, p<0.001), F(M) group (65.875 ± 36.884 μm, p<0.05), T+F(M) group (159.875 ± 32.783 μm, p<0.001) and T(M+L) group (118.750±23.939 μm, p<0.001) (Figure 3B), respectively. The area of calcified cartilage thickness varied significantly in OA knee (Figure 3A). ESWT significantly increased the calcified cartilage thickness with the thickest cartilages from 143 μm to 221 μm in T(M), F(M), T+F(M) and T(M+L) groups. There was, however, no significant difference among the ESWT groups in OA knee (Figure 3C). These results indicated that the level of cartilage degeneration was protected by ESWT on different locations and T+F(M) group had better topographical variation of articular cartilage in ESWT groups.
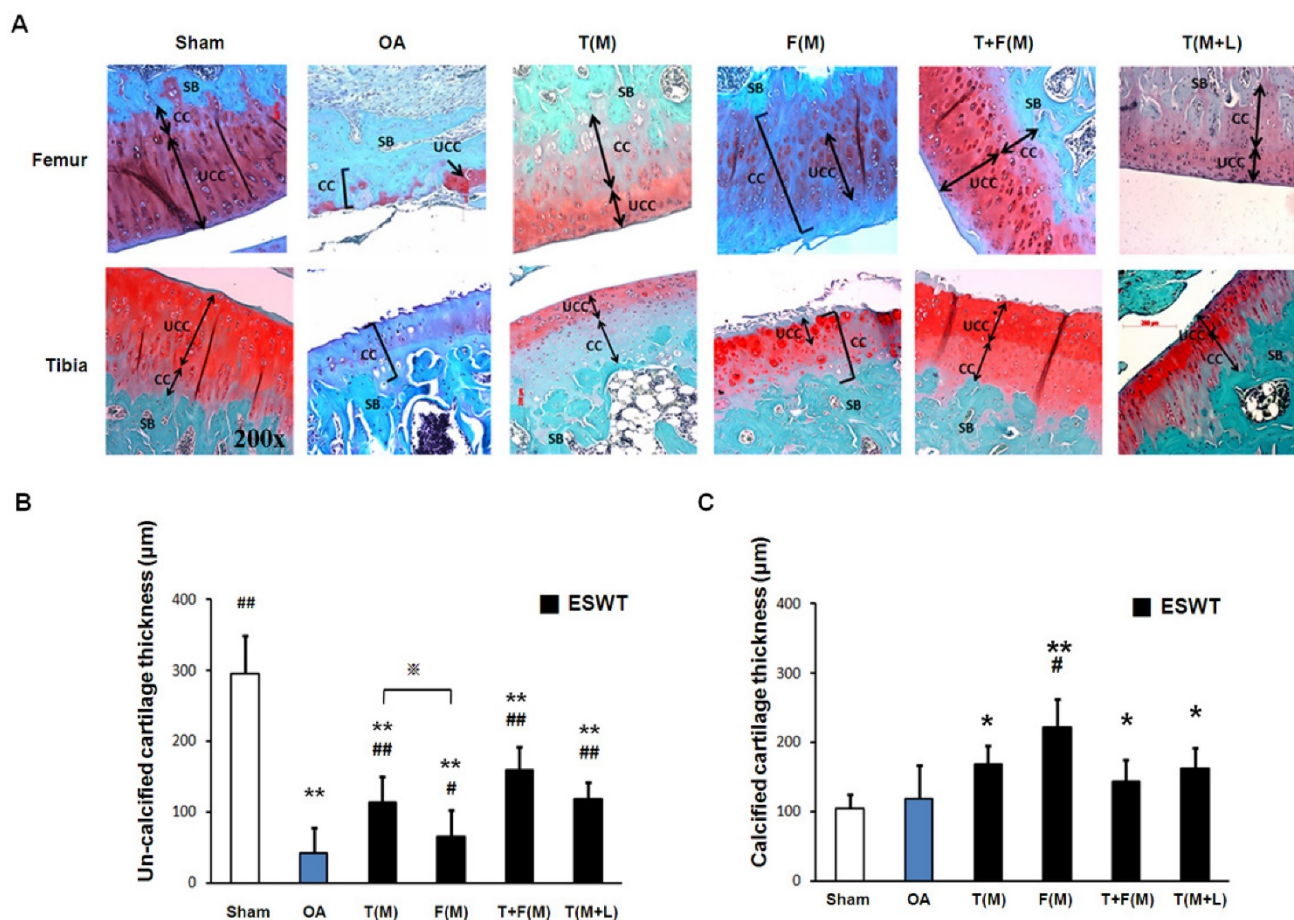

Figure 3. The microphotographs showed un-calcified and calcified cartilages of the knee. (A) Microphotographs of the distal femur and proximal tibia showed un-calcified and calcified cartilage thickness in different groups. The magnification of the image was ×200. (B), (C) Graphic illustrations of un-calcified and calcified cartilage thickness in different groups were showed in this study. The ESWT groups showed significant increasing in un-calcified cartilage and decreasing in calcified cartilage. *P < 0.05, **P < 0.001 compared to sham group. #P < 0.05, ##P < 0.001 compared to OA group. ※P < 0.05 compared to T(M) group. All rats were n = 8.
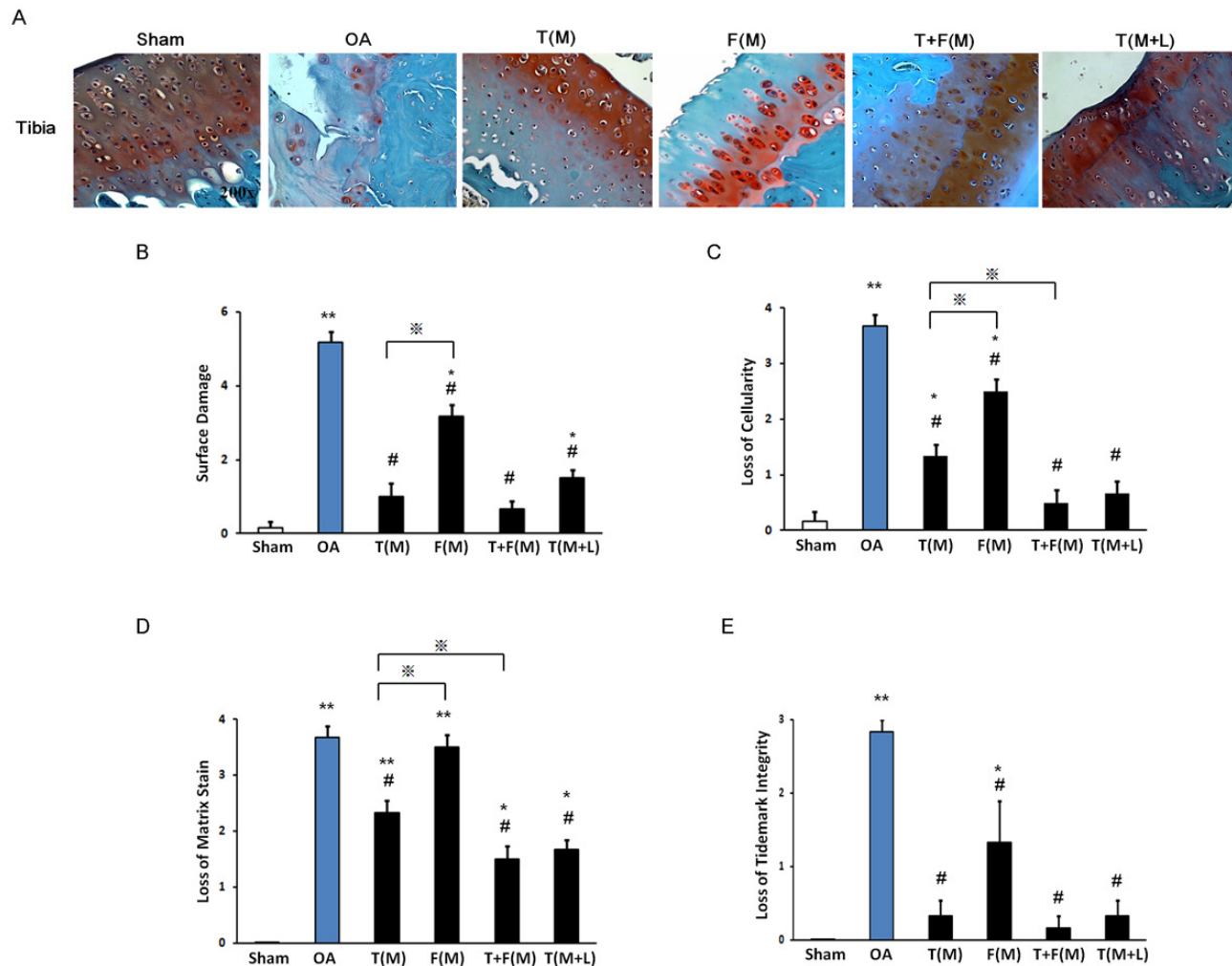
Figure 4. The histopathology of cartilage assessment. The cartilage histopathology was measured from articular cartilage of the tibia by Safranin-O stain (A). The surface damage (B), the loss of cellularity (C), the loss of matrix stain (D) and the loss of tidemark integrity were measured. *P < 0.05, **P < 0.001 compared to sham group. #P < 0.05, ## P < 0.001 compared to OA group. ※P< 0.05 compared to T(M) group. All rats were n = 8.

The effects of ESWT in subchondral bone remodeling and cartilage repair

The micro-CT analyses in sagittal and transverse planes were shown in Fig 5A. The bone volume, bone porosity, trabecular thickness and trabecular number were measured individually (Figures 5B, 5C, 5D and 5E). The micro-CT data showed significant decrease in bone volume (57.768 ± 1.961 vs 37.260 ± 2.969 %, p<0.001) and trabecular number (4.417 ± 0.183 vs 2.968 ± 0.287 per mm, p<0.001) and an increase in bone porosity (36.375 ± 1.247 vs 52.956 ± 6.043 %, p<0.001) and trabecular thickness (173.257 ± 21.126 vs 252.488 ± 28.550 μm, p<0.001) in sham group relative to OA group. ESWT groups significantly increased bone volume (60.882 ± 6.638 to 70.540 ± 3.824 % vs 37.260 ± 2.696 % per mm, p<0.001) and trabecular number (3.225 ± 0.436 to 3.914 ± 0.119 per mm vs 2.968 ± 0.287 per mm, p<0.001) and a decrease in bone porosity (38.527 ± 3.076 to 27.092 ± 4.128 % vs 52.956 ± 6.043 %, p<0.05) and trabecular thickness

(273.217 ± 18.352 to 211.701 ± 12.239 μm vs 252.488 ± 28.550 μm, p<0.05) compared to OA group. However, there were no significant differences among ESWT groups in bone remodeling. In BMD measurement, the data showed significant decrease in OA group relative to the sham group (data not shown) [30]. ESWT significantly increased the BMD values with compatible data in T(M), F(M), T+F(M) and T(M+L) groups and no significant difference was noted after ESWT.

The immunohistochemical analyses and the molecular expressions of TUNEL, PCNA and CD31 were surveyed in Figures 6A, 6B and 6C, respectively. The significant decreases of PCNA (21.468 ± 2.810 vs 1.980 ± 1.519 %, p<0.001) and increases activity of TUNEL (5.758 ± 1.108 vs 80.713 ± 9.432 %, p<0.001) and CD31 (0.141 ± 0.220 vs 1.896 ± 0.204, p<0.001) were observed in sham group relative to the OA group. The percentage of TUNEL-positive cells were reduced in T(M) (14.139 ± 4.960 %, p<0.001), T+F(M) (7.469 ± 1.211

%, p<0.001) and T(M+L) (14.301±3.277 %, p<0.001) groups as compared to OA group (80.731±9.432) (Figure 6A). ESWT significantly increased PCNA positive cartilage cells in T(M) (58.324±14.986 %, p<0.001), T+F(M) (79.152±5.050 %, p<0.001) and T(M+L) (62.308±9.347 %, p<0.001) groups compared to OA group (Figure 6B). In particular, T+F(M) was highest than other ESWT groups to stimulate cartilage cell proliferation. We observed vascular invasion was suppressed by CD31 expression in T(M) (0.976±0.105, p<0.001), T+F(M) (0.713±0.086, p<0.001), and T(M+L) (0.983±0.132, p<0.001) groups as compared to OA group (1.896±0.204) (Figure 6C). Therefore, the most positive effects for observation of specific markers after ESWT was located at T+F(M).
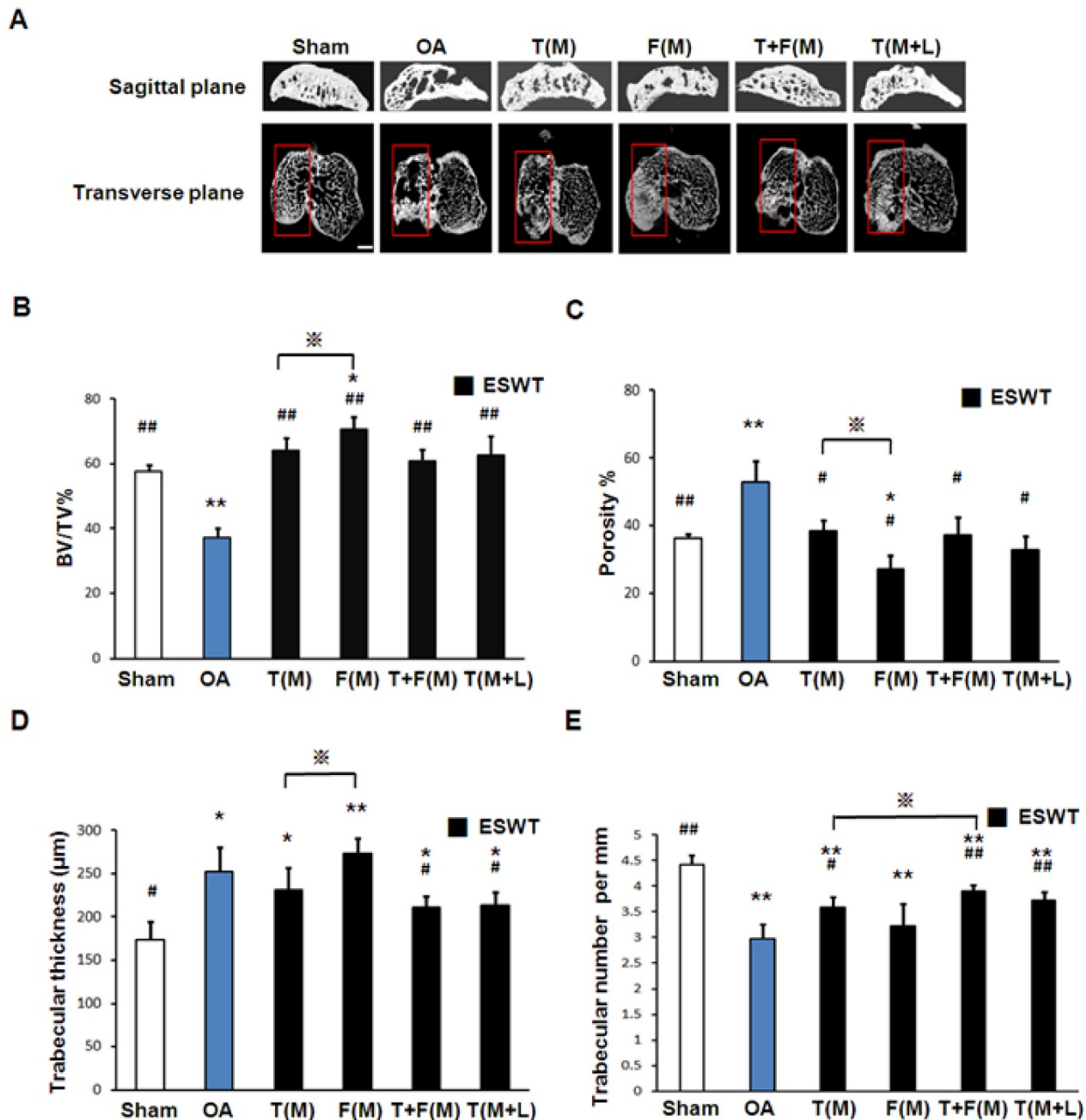

Figure 5. Photographs showed micro-CT scan of proximal tibia in different groups. (A) The result showed photomicrographs of the knee in saggital and transverse views from micro-CT. The subchondral bone medial compartment of each group was marked (red box). The scale bar represented 1 mm and rats n = 3. (B), (C), (D) and (E) showed the graphic illustrations of bone volume, bone porosity, trabecular bone thickness and trabecular number in different groups. ESWT groups showed significant increases in bone volume, and trabecular numbers, and decrease in bone porosity and trabecular thickness as compared to sham group and OA group. *P < 0.05, **P < 0.001 compared to sham group. #P < 0.05, ##P < 0.001 compared to OA group. ※P < 0.05 compared to T(M) group. All rats were n = 8.
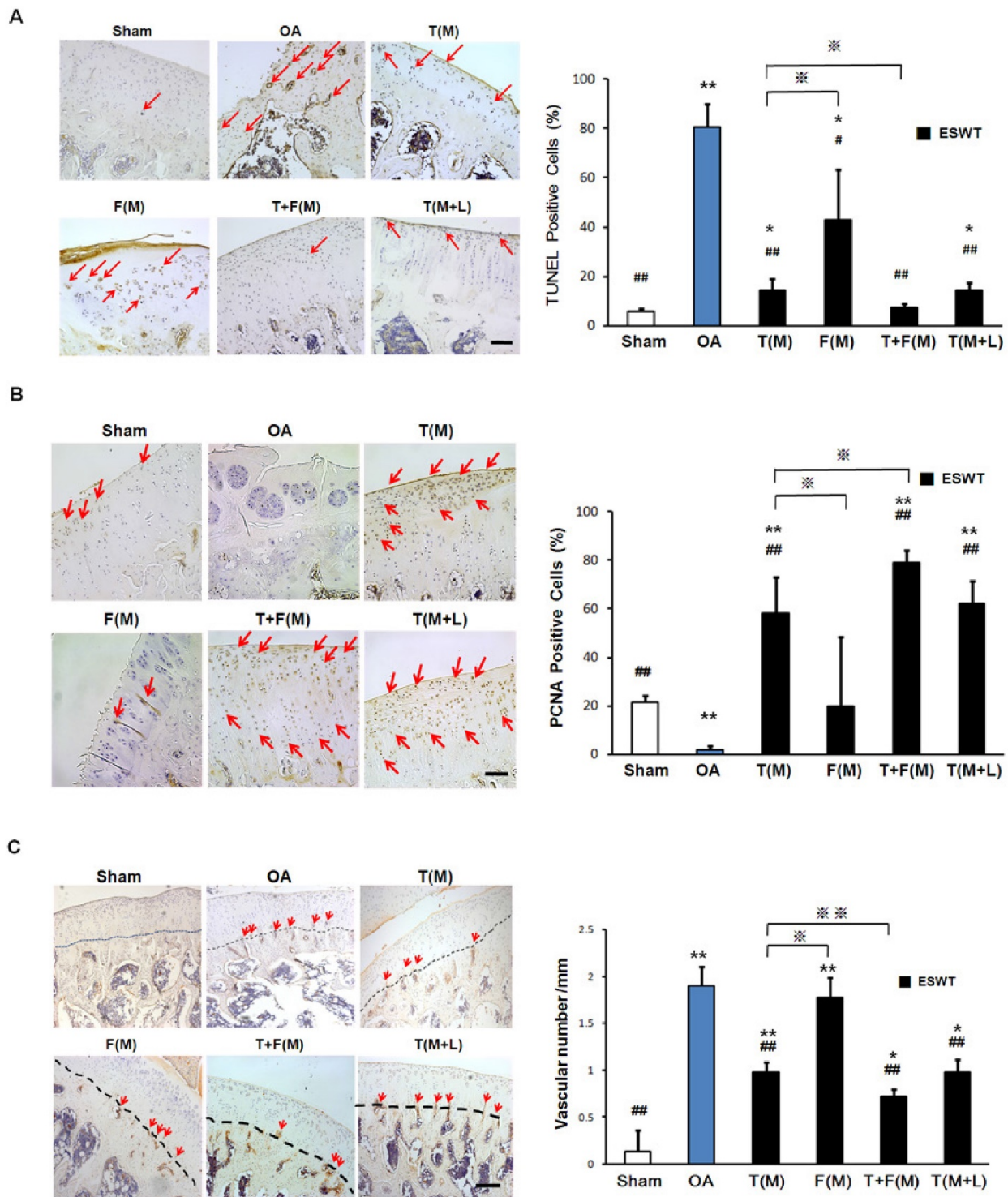
Figure 6. Immunohistochemical analysis for molecular changes on different positions with ESWT. Microscopic features of immunohistochemical stains (left) and quantification (right) showed the effect of TUNEL assay (A) and the expression levels of PCNA (B) and CD31 (C) after ESWT on different positions. *$P < 0.05$, **$P < 0.001$ compared to sham group. #$P < 0.05$, ##$P < 0.001$ compared to OA group. ※$P < 0.05$, ※※$P < 0.001$ compared to T(M) group. All rats were n = 8. The scale bar represented 100 μm.

Discussion

Prior studies demonstrated that the changes in subchondral bone characteristics may play an important role in the development of osteoarthritis of the knee [4-6]. Other studies emphasized that subchondral bone should be the major target for the treatment of pain and disease progression in OA knee [12]. The results of the current study showed that application of shockwave to the subchondral bone

was effective to ameliorate the knee from developing OA knee after ACLT and MM in rats. Furthermore, application of ESWT to the subchondral bone of the medial tibia condyle of the knee resulted in the most chondroprotective effects as compared to other locations that may also prevent the knee from developing osteoarthritis in ACLT and MM animal knee models.

The major findings in this study confirmed that ESWT is chondroprotective, and the effects appeared to be treatment location sensitive. Overall, application of ESWT to the medial tibia and femur condyles showed better chondroprotective results as compared with previous study of medial tibia and other locations of the knee in this experiment. The results of this study were in agreement with the results of previous studies that ESWT had chondroprotective effects in osteoarthritis of the knee [23, 24, 31-33]. However, the exact location-sensitive effects of ESWT in osteoarthritis of the knee were not previously reported. Our findings provided the basic data in the use of animal model in research and offer guidance in clinical application when ESWT is chosen for knees with early osteoarthritis.

The exact mechanism of ESWT remains unknown. Prior studies showed that ESWT may act as a mechanotransduction that produced biological responses to the target tissues by anti-inflammation, promotion of cell proliferation and stimulation of the ingrowth of neovascularization, that in turn, results in tissue regeneration and repair such as osteoarthritis of the knee [34, 35]. Other studies also reported that ESWT reduced pain and improved function of the knee by suppression of substance P positive nerve fibers from dorsal neuron ganglion to the knee and calcitonin-gene related peptide around the knee [21]. The results of the current study confirmed that application of ESWT to the subchondral bone of the medial tibia and femur condyle yields the most effects in the initiation of osteoarthritis of the knee, and ESWT showed location-sensitive effects in osteoarthritis after ACLT +MM knees in rats.

Conclusions

ESWT is effective in the prevention on the initiation of ACLT and MM induced osteoarthritis of the knee in rats. We expanded our previous study and detail described the pathological changes in articular cartilage and subchondral bone. ESWT showed the site-sensitive and location-specific with the best results when ESWT are simultaneously applied to medial distal femur and proximal tibia.

Supplementary Material

Supplemental figure 1.
http://www.medsci.org/v14p0213s1.pdf

Acknowledgments

Conflicts of Interest

The authors declared that they did not receive any honoraria or consultancy fees in writing this manuscript. No benefits in any form have been received or will be received from a commercial party related directly or indirectly to the subject of this article. One author (Ching-Jen Wang) serves as a member of the advisory committee of Sanuwave, (Alpharetta, GA) and this study is performed independent of the appointment. The remaining authors declared no conflict of interest.

References

1. Michael JW, Schluter-Brust KU, Eysel P. The epidemiology, etiology, diagnosis, and treatment of osteoarthritis of the knee. Dtsch Arztebl Int. 2010; 107: 152-62.
2. Lane NE, Nevitt MC. Osteoarthritis, bone mass, and fractures: how are they related? Arthritis Rheum. 2002; 46: 1-4.
3. Oettmeier R, Abendroth K. Osteoarthritis and bone: osteologic types of osteoarthritis of the hip. Skeletal Radiol. 1989; 18: 165-74.
4. Burr DB, Schaffler MB. The involvement of subchondral mineralized tissues in osteoarthrosis: quantitative microscopic evidence. Microsc Res Tech. 1997; 37: 343-57.
5. Burr DB. The importance of subchondral bone in osteoarthrosis. Curr Opin Rheumatol. 1998; 10: 256-62.
6. Radin EL, Rose RM. Role of subchondral bone in the initiation and progression of cartilage damage. Clin Orthop Relat Res. 1986: 34-40.
7. Dedrick DK, Goulet R, Huston L, Goldstein SA, Bole GG. Early bone changes in experimental osteoarthritis using microscopic computed tomography. J Rheumatol Suppl. 1991; 27: 44-5.
8. Hayami T, Funaki H, Yaoeda K, Mitui K, Yamagiwa H, Tokunaga K, et al. Expression of the cartilage derived anti-angiogenic factor chondromodulin-I decreases in the early stage of experimental osteoarthritis. J Rheumatol. 2003; 30: 2207-17.
9. Hayami T, Pickarski M, Zhuo Y, Wesolowski GA, Rodan GA, Duong LT. Characterization of articular cartilage and subchondral bone changes in the rat anterior cruciate ligament transection and meniscectomized models of osteoarthritis. Bone. 2006; 38: 234-43.
10. Muraoka T, Hagino H, Okano T, Enokida M, Teshima R. Role of subchondral bone in osteoarthritis development: a comparative study of two strains of guinea pigs with and without spontaneously occurring osteoarthritis. Arthritis Rheum. 2007; 56: 3366-74.
11. Hayami T, Pickarski M, Wesolowski GA, McLane J, Bone A, Destefano J, et al. The role of subchondral bone remodeling in osteoarthritis: reduction of cartilage degeneration and prevention of osteophyte formation by alendronate in the rat anterior cruciate ligament transection model. Arthritis Rheum. 2004; 50: 1193-206.
12. Dieppe P. Subchondral bone should be the main target for the treatment of pain and disease progression in osteoarthritis. Osteoarthritis Cartilage. 1999; 7: 325-6.
13. Brama PA, TeKoppele JM, Bank RA, Barneveld A, van Weeren PR. Biochemical development of subchondral bone from birth until age eleven months and the influence of physical activity. Equine Vet J. 2002; 34: 143-9.
14. Ratcliffe A, Seibel MJ. Biochemical markers of osteoarthritis. Curr Opin Rheumatol. 1990; 2: 770-6.
15. Richmond J, Hunter D, Irrgang J, Jones MH, Levy B, Marx R, et al. Treatment of osteoarthritis of the knee (nonarthroplasty). J Am Acad Orthop Surg. 2009; 17: 591-600.
16. Hochberg MC, Altman RD, April KT, Benkhalti M, Guyatt G, McGowan J, et al. American College of Rheumatology 2012 recommendations for the use of

nonpharmacologic and pharmacologic therapies in osteoarthritis of the hand, hip, and knee. Arthritis Care Res (Hoboken). 2012; 64: 465-74.

17. Petrella RJ. Hyaluronic acid for the treatment of knee osteoarthritis: long-term outcomes from a naturalistic primary care experience. Am J Phys Med Rehabil. 2005; 84: 278-83; quiz 84, 93.

18. Dahlberg J, Fitch G, Evans RB, McClure SR, Conzemius M. The evaluation of extracorporeal shockwave therapy in naturally occurring osteoarthritis of the stifle joint in dogs. Vet Comp Orthop Traumatol. 2005; 18: 147-52.

19. Frisbie DD, Kawcak CE, McIlwraith CW. Evaluation of the effect of extracorporeal shock wave treatment on experimentally induced osteoarthritis in middle carpal joints of horses. Am J Vet Res. 2009; 70: 449-54.

20. Mueller M, Bockstahler B, Skalicky M, Mlacnik E, Lorinson D. Effects of radial shockwave therapy on the limb function of dogs with hip osteoarthritis. Vet Rec. 2007; 160: 762-5.

21. Ochiai N, Ohtori S, Sasho T, Nakagawa K, Takahashi K, Takahashi N, et al. Extracorporeal shock wave therapy improves motor dysfunction and pain originating from knee osteoarthritis in rats. Osteoarthritis Cartilage. 2007; 15: 1093-6.

22. Revenaugh MS. Extracorporeal shock wave therapy for treatment of osteoarthritis in the horse: clinical applications. Vet Clin North Am Equine Pract. 2005; 21: 609-25, vi.

23. Wang CJ, Weng LH, Ko JY, Sun YC, Yang YJ, Wang FS. Extracorporeal shockwave therapy shows chondroprotective effects in osteoarthritic rat knee. Arch Orthop Trauma Surg. 2011; 131: 1153-8.

24. Wang CJ, Sun YC, Wong T, Hsu SL, Chou WY, Chang HW. Extracorporeal shockwave therapy shows time-dependent chondroprotective effects in osteoarthritis of the knee in rats. J Surg Res. 2012; 178: 196-205.

25. Hayami T, Pickarski M, Zhuo Y, Wesolowski GA, Rodan GA, Duong le T. Characterization of articular cartilage and subchondral bone changes in the rat anterior cruciate ligament transection and meniscectomized models of osteoarthritis. Bone. 2006; 38: 234-43.

26. Glasson SS, Chambers MG, Van Den Berg WB, Little CB. The OARSI histopathology initiative - recommendations for histological assessments of osteoarthritis in the mouse. Osteoarthritis Cartilage. 2010; 18 Suppl 3: S17-23.

27. Pastoureau P, Leduc S, Chomel A, De Ceuninck F. Quantitative assessment of articular cartilage and subchondral bone histology in the meniscectomized guinea pig model of osteoarthritis. Osteoarthritis Cartilage. 2003; 11: 412-23.

28. Pritzker KP, Gay S, Jimenez SA, Ostergaard K, Pelletier JP, Revell PA, et al. Osteoarthritis cartilage histopathology: grading and staging. Osteoarthritis Cartilage. 2006; 14: 13-29.

29. Wang CJ, Weng LH, Ko JY, Wang JW, Chen JM, Sun YC, et al. Extracorporeal shockwave shows regression of osteoarthritis of the knee in rats. J Surg Res. 2011; 171: 601-8.

30. Wang CJ, Sun YC, Siu KK, Wu CT. Extracorporeal shockwave therapy shows site-specific effects in osteoarthritis of the knee in rats. J Surg Res. 2013; 183: 612-9.

31. Wang CJ, Hsu SL, Weng LH, Sun YC, Wang FS. Extracorporeal shockwave therapy shows a number of treatment related chondroprotective effect in osteoarthritis of the knee in rats. BMC Musculoskelet Disord. 2013; 14: 44.

32. Wang C-J, Sun Y-C, Wu C-T, Weng L-H, Wang F-S. Molecular changes after shockwave therapy in osteoarthritic knee in rats. Shock Waves. 2013; 26: 45-51.

33. Wang CJ, Huang CY, Hsu SL, Chen JH, Cheng JH. Extracorporeal shockwave therapy in osteoporotic osteoarthritis of the knee in rats: an experiment in animals. Arthritis Res Ther. 2014; 16: R139.

34. Wang CJ, Wang FS, Yang KD, Weng LH, Hsu CC, Huang CS, et al. Shock wave therapy induces neovascularization at the tendon-bone junction. A study in rabbits. J Orthop Res. 2003; 21: 984-9.

35. Cheng JH, Wang CJ. Biological mechanism of shockwave in bone. Int J Surg. 2015; 24: 143-6.